# Effect of leaflet asymmetry on mechanical properties of lipid bilayers with phosphatidic acid

Dominik Drabik[a,b*], Piotr Hinc[a], Mareike Stephan[b], Aleksander Czogalla[a*] and Rumiana Dimova[b*]

[a] Faculty of Biotechnology, University of Wroclaw, F. Joliot-Curie 14a, 50-383 Wroclaw, Poland
[b] Max Planck Institute of Colloids and Interfaces, Science Park Golm, 14476 Potsdam, Germany
[*] Correspondence –Dominik Drabik (Dominik.Drabik@UWr.edu.pl), Aleksander Czogalla (Aleksander.Czogalla@UWr.edu.pl) & Rumiana Dimova (Rumiana.Dimova@mpikg.mpg.de)

**ABSTRACT :** Asymmetry in membranes strongly affects their biophysical characteristics and behaviour. It is a very important factor to consider for understanding the functioning of membranes in biological systems, especially in regards to lipid molecules that are known to localize in one leaflet over the other. Phosphatidic acid is one representative of this family of molecules. Reported to play a crucial role in lipid metabolism and suspected to participate in cellular signalling, its specific nature might only be exhibited in asymmetric systems. Here, using giant unilamellar vesicles, we studied two asymmetric phosphocholine-based bilayer systems with 1-palmitoyl-2-oleoyl phosphatidic acid (POPA) localized in either the inner or the outer membrane leaflet. We systematically characterized and compared the investigated systems to their symmetric counterpart. To verify and quantify the presence of POPA in the membrane, α-synuclein-mEGFP was used. We report an increase in the area compressibility and bending rigidity moduli in the asymmetric membranes compared to the symmetric ones. Furthermore, we show area compressibility differences depending on the localization of POPA in the leaflets. The results suggest the asymmetry affects both mechanics and phase state of the membrane.

## 1. Introduction

Lipid vesicles models are commonly used to study the behavior and dynamics taking place in biological membranes. Among them, giant vesicles represent a convenient system to directly explore and visualize the membrane under a microscope [1, 2]. As simplified biological membranes often formed with a spherical shape, they can be employed to assess various membrane characteristics regarding lipid dynamics, properties and organization [3]. For instance, they have been successfully used for cell function studies [4-6], as artificial tissue models [7] and for resolving protein-lipid interactions [8], to list a few. However, one of the biggest difference between biological membranes and the membrane of lipid vesicles as investigated in a large bulk of studies is the lack of asymmetry in the latter. In living cells, asymmetry was reported to be a prevalent and fundamental feature [9-11]. While advances in lipidomics showed the presence of a variety of lipids, their lateral distribution still remains poorly understood. The biophysical consequences of membrane asymmetry remain poorly explored. However, asymmetry could be a crucial factor to understand the functioning of lipid molecules that are known to be present in only one of the membrane leaflets.

One of such lipid type is the phosphatidic acid (PA). Phosphatidic acids are characterized by a negative charge, presence of a phosphomonoester group and, compared to other membrane lipids, by a relatively small head group. PAs play a crucial role in lipid metabolism, as they are used in the synthesis of all other types of glycerophospholipids and act as a modulator of membrane shape [12, 13]. However, compared to pure phosphatidylcholine (PC) membranes, symmetric models of membranes containing various types of PA have not shown differences specific to the PA lipid type [14]. Nevertheless, in biological systems, PA were reported to localize only within the inner leaflet of erythrocyte membranes [9, 15]. Furthermore, PA-producing enzymes, such as diacylglycerol kinase, were reported to localize only on one of the leaflets of the plasma membrane and subcellular structures [16, 17]. For this reason, the characterization of asymmetric model systems, and comparison to their symmetric counterparts, could provide important information. In this work, we focus on assessing the mechanical properties of such membranes.

Progress towards understanding asymmetric membranes using giant vesicles has been initiated with the introduction of methods for their preparation. The most common and still most-widely used method for production of GUVs with asymmetric leaflets is the phase-transfer method (also known as oil droplet or emulsion transfer), first introduced by Träuble and Grell [18] and later employed in various reports [19-23]. The approach relies on the formation of each leaflet separately, followed by their assembly under external force (from gravitation, centrifugation or microfluidic flow). The first protocols involves the preparation of water-in-oil emulsion (aqueous phase dispersed in a nonpolar solvent, i.e. oil) stabilized by lipids forming a monolayer at the droplet surface. Then, the droplets get covered by a second lipid layer by applying small force pulling them through another oil-water interface (stabilized by the lipid on the outer leaflet) to obtain the vesicle architecture . Alternative approaches to generate GUVs with asymmetric membrane composition are based on hemifusion [24], cyclodextrin-mediated lipid exchange [25, 26] and microfluidic jetting [27, 28].

There are only a few reports studying the mechanical properties of asymmetric lipid membranes. These include the studies of bending rigidity of POPC/DOPC asymmetric vesicles obtained via the phase transfer method [29]. The reported value of bending rigidity was almost twice the value of corresponding symmetric systems. Similar effect was confirmed with another study in which the asymmetric vesicles were obtained with a microfluidic device [28]. A study, investigating DMPC/DOPC vesicles obtained using custom-made microfluidic devices [30], reported increased bending rigidity and area compressibility for the investigated asymmetric system compared to the symmetric ones.

In this work, we investigate the mechanical properties of asymmetric POPC:POPA membranes. For completeness, we examine systems in which POPA is located either in the inner or the outer leaflet. Furthermore, we compare the asymmetric GUV systems to symmetric ones obtained with two different method to eliminate any possible influence of the preparation approach. To ensure that the reported phenomena are not induced by poor knowledge of the system composition, we systematically characterized the obtained vesicles with various approaches such as the use of α-synuclein-mEGFP as a PA sensor. This protein was already reported to strongly bind to membranes with PA fractions [31, 32]. Using micropipette aspiration, we probe the mechanical properties of the different systems in terms of bending rigidity and stretching elasticity and discuss the resolved differences of the symmetric versus the asymmetric system.

## 2. Materials and methods

### 2.1 Materials

Lipids POPC (1-palmitoyl-2-oleoyl-glycero-3-phosphocholine) and POPA (1-palmitoyl-2-oleoyl-sn-glycero-3-phosphatidic acid) and fluorescent probe NBD-PC were purchased from Avanti Polar Lipids (Alabaster, AL, USA). Fluorescent probe TexasRed-DHPE was purchased from Invitrogen (Waltham, MS, USA). Sucrose, glucose, imidazole, TEMED (N,N,N′,N′-Tetramethyl ethylenediamine), lysozyme from chicken egg white and Sigma mineral oils were purchased from Sigma Aldrich (international). Roth mineral oil, IPTG (Isopropyl-β-D-thiogalactopyranosid), TRIS (Tris-(hydroxymethyl)-amino methane), PMSF (phenylmethyl sulphonyl fluoride), Triton® X-100, HEPES (N-2-Hydroxyethylpiperazine-N'-2-ethane sulphonic acid) and Rotiphorese® Gel 30 were purchased from Roth (international). Restriction enzymes EcoRI-HF, BamHI-HF, DpnI, as well as Phusion® High-Fidelity DNA Polymerase and Quick Ligation™ Kit were purchased from NEB (Ipswich, MS, USA). Ultrapure dNTPs Mix, AGAROSE Electrophoresis grade and OMNI Nuclease were purchased from EURx (Poland). NucleoSpin® Plasmid isolation kit and NucleoSpin® Gel and PCR Clean-up kit were purchased from Macherey-Nagel (Germany). PierceTM Protease Inhibitor Tablets EDTA free and Pierce™ High Capacity Ni-IMAC Resin were purchased from Thermo Scientific (international). Glycerol, sodium chloride and ammonium persulfate were purchased from POCH (Poland). LB Miller Broth was purchased from IBI Scientific (international). Kanamycin Sulfate was purchased from BioShop (Poland). pET3a aSyn murine was gifted from Gabriele Kaminski Schierle (Addgene plasmid #108865).

### 2.2 Vesicle preparation

Both asymmetric and symmetric vesicles were obtained using reverse oil-transfer method (sometimes described as inverted emulsion method) [33]. This requires lipid to first be dissolved in oil. To prepare lipid-in-oil solutions, lipid was dissolved in chloroform which was then removed under the stream of nitrogen and followed by keeping the samples in vacuum for 1 h. Oil was added so the concentration of lipid in oil solutions was equal to 400 µM, which was followed by sonication for 60 minutes. Sigma mineral oil was used as the interphase oil (for outer leaflet), while Roth mineral oil was used as an emulsion oil (for inner leaflet). Oils were selected in such a way to obtain the purest vesicles and the biggest yield. This was followed by interfacial incubation. Sequentially, 250 µL of 700mOsm glucose and 200 µL of interphase lipid-oil solution was added to Eppendorf protein LoBind tubes. The system was left for 3h to form the interfacial lipid layer. After that the system was centrifuged for 5 minutes at 600×G to ensure sufficient layer formation. This was followed by preparation of droplet emulsion. Specifically, sucrose solution (700mOsm) was added to emulsion oil in ratio 1 µL of sucrose to 50 µL of oil. Water-oil emulsion was achieved by performing a series of sequential rubbing to form fine lipid droplets. The emulsion was put slowly on the top of the water/oil tube and centrifuged at 130×G for 10 minutes. All preparation steps were performed at room temperature (24 °C).

For electroformation of control vesicles standard electroformation protocol was used. Briefly, 4 µl of 4 mM POPC or POPC/POPA mixture and fluorescent probe mixture (0.2m%) in chloroform was distributed equally along the ITO glass coverslips and dried under the vacuum for 1 hour. The coverslips were set opposite to each other and the space between them was filled with 150 mOsm sucrose. This was followed by appliance of 10 Hz AC electric field for 2 h with 1V voltage and 1 Hz frequency. Electroformation was carried out at 30 °C.

### 2.3 Expression and purification of α-synuclein

To obtain plasmid construct for overexpression of 8×His - tagged murine α-synuclein fused with mEGFP (monomeric enhanced green fluorescent protein) in bacterial system, first coding sequence of N-terminal (Met1 – Lys60) α-synuclein fragment was amplified and subcloned from pET3a aSyn murine to pET28 plasmid containing mEGFP coding sequence by doble restriction digest (BamHI and EcoRI enzymes) and ligation according to manufacturer protocols. Then Restriction Free Cloning method was performed to clone the rest of the α-synuclein sequence into the previously prepared construct and obtain a plasmid encoding the complete α-synuclein sequence fused to mEGFP. The Restriction Free Cloning procedure was performed according to the instruction described by van den Ent & Löwe [34] using the primers designed in https://www.rf-cloning.org/tool. To confirm and validate performed cloning, the obtained DNA constructs were subjected to Sanger sequencing with primers specific to T7 promoter and T7 terminator sequence (Microsynth Seqlab GmbH, Germany). The sequences of the primers used in the cloning procedures are provided in the Supplementary Materials Section 1.
Production of recombinant α-synuclein-mEGFP protein was performed in Escherichia coli NiCo21 (DE3) strain. 200 ml of kanamycin supplemented LB Miller broth was inoculated with overnight preculture and incubated at 37 °C with 200 rpm agitation to reach culture optical density (λ=600 nm) of 0,7. Then the protein overexpression was induced by adding IPTG at the final concentration of 400 µM. Protein overexpression was carried out at 18 °C with 200 rpm agitation for 18 hours. Next cells were harvested by centrifugation (10.000×g, 20 min, 4 °C) and lysed by resuspending pellet in 10 ml of Lysis Buffer (10 mM HEPES, 500 mM NaCl, 1 mg/ml lysozyme, 0,75% Triton X-100, 25 U/ml OMNI Nuclease, 10 mM imidazole, 1 mM PMSF, 1× Price$^{TM}$ Protease Inhibitor Tablets EDTA free, pH 8.0) and subsequent incubation for 1h at 4 °C with gentle mixing. Afterwards the suspension was sonicated on ice for 15 minutes at 80% amplitude and 0.5 cycle (Hielscher UP100H Ultrasonic Processor with MS3 sonotrode). Lysate was then clarified by centrifugation (35,000×g, 30 min, 4 °C) and the supernatant was incubated with 1 ml of previously equilibrated PriceTM High Capacity Ni-IMAC resin for 2 h at 4 °C with gentle mixing. Resin was packed into a chromatography column and washed with 100 ml of Wash Buffer 1 (10 mM HEPES, 500 mM NaCl, 10 mM imidazole, 20% glycerol, pH 8.0), 100 ml of Wash Buffer 2 (10 mM HEPES, 300 mM NaCl, 10 mM imidazole, 20% glycerol, pH 8.0) and with Wash Buffer 3 (10 mM HEPES, 300 mM NaCl, 10 mM imidazole, pH 8.0) until the absorbance (λ=280 nm) of flow through buffer decreased to < 0,01. Then protein was eluted from resin with Elution Buffer (10 mM HEPES, 300 mM NaCl, 200 mM imidazole, pH 8.0). Eluted fractions was then dialyzed against 10 mM HEPES + 150 mM NaCl buffer pH 7.4 and the protein concentration was determined spectrophotometrically (Cary 1E UV-Visible Spectrophotometer) employing excitation coefficient calculated using ProtParam Expasy tool (web.expasy.org/protparam). Purity and molecular weight of produced protein was determined by Tris-glycine SDS-PAGE in Laemmli system with the following Coomasie Brilliant Blue R-250 staining. The SDS-Page analysis is presented in Supporting Figure S1.

### 2.4 Fluorescence quantification

The fluorescence quantification of NBD-PC dye was done on Leica SP8 (Leica, Germany) confocal microscope. 512 px × 512 px fluorescent images were collected. Identical acquisition setting (constant zoom, laser intensity, detector gain) were maintained for all measurements. Samples were illuminated at 488 nm. The fluorescence quantification of αSyn-mEGFP was performed similarly. The vesicles in equiosmolar solution were diluted twice with glucose/300mM NaCl solution so the final concentration of NaCl in the sample was equal to 150mM. This was followed by addition of the αSyn-mEGFP to a final concentration of 500 nM and 5 minutes incubation to ensure equal distribution of the protein within the sample. The concentration of protein was previously optimized following the intensity dependence on the concentration of PA in the membrane (see Supporting Information Section 3, Figure S2). The fluorescence intensity at the GUV membrane was calculated using Circle Skinner add-on to ImageJ (github.com/tinevez/CircleSkinner).

### 2.5 Zeta-potential measurements

Zeta potential measurements on GUVs were done according to already established protocols [35, 36] using Malvern ZetaSizer NanoZS (Malvern, UK). Briefly, GUVs were measured in both dip-cell/u-cells with electrophoretic movement set to 150/10 V in the instrumental settings. The sample is measured not more than 3 times (repeated measurements can result in GUV rupture at the electrodes). Based on the output quality report, poor results were discarded. At least 3 independently obtained populations were measured to ensure the reproducibility of the reported values. For series of measurements at pH 7.4, the selected buffer was 5 mM HEPES adjusted with KOH.

### 2.6 Micropipette aspiration technique

Micropipettes (inner diameter 5–10 um) were prepared from glass capillaries (World Precision Instruments, Sarasota, FL, USA) with the use of a micropipette puller (Sutter Instruments USA, Novato, CA) and their tips were shaped with a microforge (Narishige, Tokyo, Japan). Before use, each micropipette was coated with 1 mg/ml caseine solution to prevent vesicle adhesion to the glass. To apply suction pressure, the micropipettes were connected to water reservoirs mounted on one linear translational stages (M-531.DD; PI, Karlsruhe, Germany). Manipulation within the sample was achieved with the use of micromanipulators (MHW-103 and MLW-3; Narishige) secured to coarse manipulators (MMN-1; Narishige). Vesicles were visualized on Leica SP5 (Leica, Germany) confocal microscopy. 1024 pixel × 1024 pixel images were collected using HCK PLAN APO 40×0.75 dry objective at 594 nm laser excitation. Length of aspiration was measured from the images using custom-written script in MATLAB.

### 2.7 Molecular dynamics simulations

The full-atomistic MD simulation was performed using NAMD 2.13 [37] software with CHARMM36 force fields [38] under NPT conditions (constant: number of particles, pressure, and temperature). Asymmetric lipid membrane systems were prepared according to surface area approach with available recommendations [39] and consisted of 652 lipid molecules (324 and 329 lipids for on each of leaflets, respectively). The system was hydrated in such a way that 75 water molecules per lipid molecule were used and was additionally neutralized with positive counter ions. The system was equilibrated using a standard equilibration procedure. Total simulation time for investigated system was 210 ns with the last 10 ns used for analysis. Simulations were carried out at ~22 °C (295 K). Membrane thickness $h_{pp}$ was calculated as the difference between mean height values of atoms in opposite leaflets for phosphorus atoms. Density profiles were plotted with VMD density profile tool [40].

### 2.8 Statistics

In order to test for the significant difference between the parameters, unless specified otherwise, the Kruskal-Wallis ANOVA test was used with the significance level at 0.05. This was followed by post hoc analysis for nonparametric test using npposthoc origin add-on. All statistical analysis was performed using the OriginPro 2015 (OriginLabs) software. Weighted average values are presented with weighted standard deviation, where weight is equal to 1/error of the measurement.

## 3. Results and Discussion

### 3.1. Asymmetry verification and composition investigation

The phase-transfer method was successfully reported to yield asymmetric GUVs [33]. However, some concerns regarding both what is the final lipid composition of the obtained vesicles and the presence of oil leftovers which may influence the properties of the systems can be raised. The latter is hinted in the literature [41]. For this reason we decided to thoroughly characterize investigated systems with both POPC and POPA lipids. We used several techniques to probe the composition of the vesicles that were subsequently used in micropipette studies. First, we employed fluorescence intensity measurements to investigated whether the vesicles exhibit asymmetry at all. This was done by adding fluorescence probe to the leaflet containing POPA and checking the fluorescence intensity of both symmetric and asymmetric vesicles. This results are presented in Figure 1A. As can be clearly concluded, the drop of intensity was around half compared to the symmetric system. This might suggest that composition asymmetry is indeed present in investigated systems. Hence, we moved to characterization of leaflet compositions. However, to characterize composition of leaflets in the lipid vesicles is not an easy task. We employed protein αSyn-mEGFP (green fluorescent protein), which was reported to strongly bind to membranes with PA and can be considered as a PA sensor [31, 32]. Results are presented in Figure 1B, where the protein was added to both asymmetric and symmetric systems, as well as to vesicles obtained by electroformation to consider any possible difference incurring from the different methods. In the case when leaflets with POPA were 'outside', the vesicles provided high fluorescence signal, in the other case there was hardly any signal at all. To provide full scope of the issue we also added αSyn-mEGFP to the aqueous phase of the water-in-oil emulsion to investigate the 'inside' of the vesicle. Similarly, when the leaflet with POPA had contact with protein, the vesicles were fluorescent, in the other case they were not. Snapshots of both vesicle types are presented in Supporting Figure S4. Given the presented results and strong non-linear intensity fluorescence signal to PA concentration dependency of αSyn-mEGFP, several conclusions can be drawn. First of all, for the time of the measurements carried in this work, which is up to 7 hours, there was no significant flip-flop of lipids – the POPA presence was limited only to one leaflet. Hence, compositional asymmetry in investigated systems is present. Secondly, the quantity of POPA in outer leaflets for both symmetric systems (obtained with electroformation and oil-transfer) as well as asymmetric one is similar.

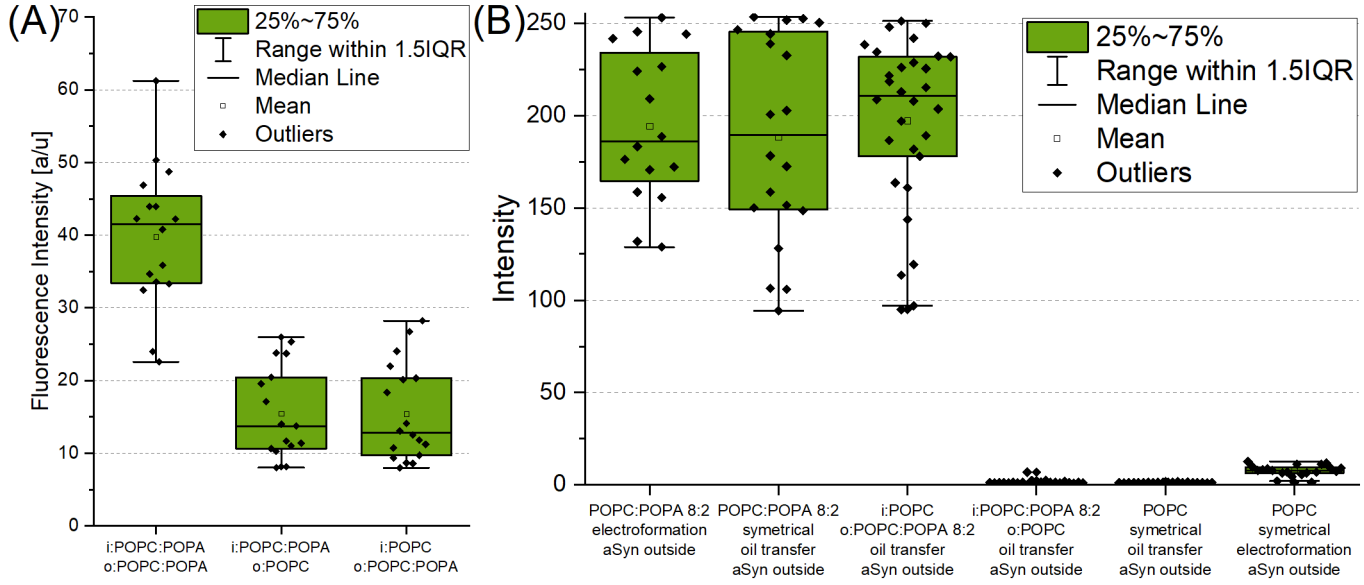


Figure 1. (A) Fluorescence quantification of both symmetric and asymmetric membrane systems in which only the POPC:POPA leaflet is labelled with 0.5 mol% NBD-PC. (B) Fluorescence quantification of investigated POPC:POPA systems with αSyn-mEGFP (500nM). All measurements were performed in RT (24 °C).

Nevertheless, we validated the above results with supporting and independent technique to ensure that drawn conclusions are correct. To this end, we employed zeta-potential measurements. While this technique is rarely used for quantification of GUVs because of associated caveats (for example, the prehistory of the GUVs is not known in terms of prior rupture and leaflet mixing), this technique was successfully used to establish zeta-potential of such vesicles [35, 36]. The results for vesicles measured in pH 7.4 HEPES are presented in Figure 2. The obtained values of zeta-potential confirm the conclusion from fluorescence quantification. Both symmetric POPC vesicles obtained from electroformation and oil-transfer, as well as asymmetric system with POPA in inner leaflet yielded convergent value of zeta-potential. Similar is the case for both POPC:POPA 80:20 systems and asymmetric system with POPA in the outer leaflet. Interestingly, zeta-potential values for neutral systems exhibited relatively high negative charge similarly to results reported in Carvalho *et al* [36]. Detailed description of measurements, as well as results for vesicles in sucrose and in the presence of 5mM NaCl and considerations for different measurement chambers are presented in Supporting Information Section

4. We believe that these results provide sufficient proof that the investigated systems are asymmetric and, at least roughly, correspond to the intended composition of the outer leaflet. Having established this we can move towards second part of vesicle characteristic – lateral organization.

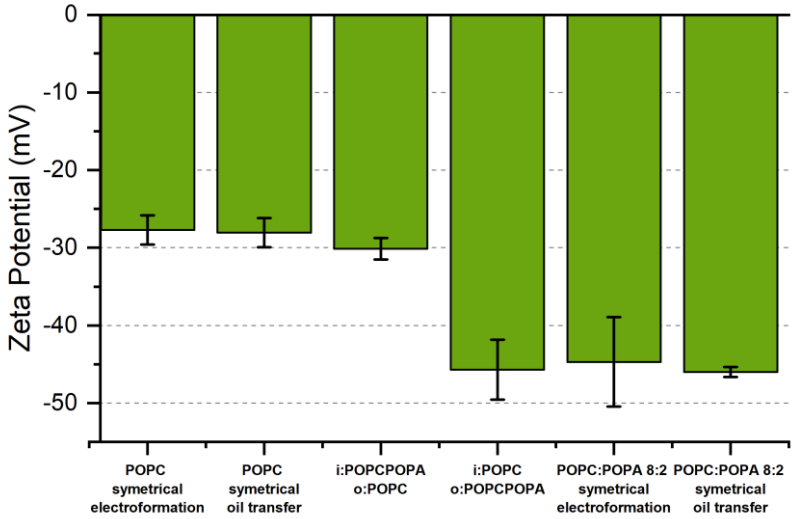


Figure 2. Zeta potential of investigated GUV systems in sucrose/glucose solution buffered with 10 mM HEPES, pH 7.4, at 25°C.

### 3.2. Gel domains presence in investigated systems

Information about the composition is only but one of the factors that needs to be considered when characterizing the membrane system. Since the transition temperature of lipid POPA is 28 °C [42], phase separation can be expected to occur in the mixed membrane systems below this temperature. Such different lateral organization might have implications to the overall mechanical properties of the investigated membranes. We used confocal microscopy to investigate the lateral organization on the membrane from Z-stacks. We observed dark gel-like domains in the symmetric POPC:POPA 80:20 membrane systems (both from electroformation and oil-transfer), as shown on Figure 3A. The gel-like nature of the domains was concluded from their shape (irregular) and stability (no shape change over time, only lateral displacement, as expected when the remaining phase is fluid). Additionally, such domains were also observed for lower concentrations of POPA, specifically POPC:POPA 95:5 and POPC:POPA 90:10 (Figure 3B), albeit slightly smaller in area. Interestingly, the gel-like domains were not observed for all of the fluorescent probes we explored. Phase separation was observed when employing fluorophores attached to DOPE (namely Atto488-DOPE, but also Rhodamine-DOPE), however for TexasRED-DHPE no domains were detected, presumably because the fluorophore did not exhibit phase preference. We believe this outcome is related to the length of acyl chains, which characterize the way the fluorescent probe behaves in terms of phase-preference. Nevertheless, for the studies of the mechanical properties, to avoid imaging artefacts, we used the dye that does not exhibit preferential phase partitioning. Interestingly, in the asymmetric system with one leaflet composed of POPC:POPA 80:20 no gel domains were observed with the phase-sensitive fluorophores. It was recently postulated that loss of plasma membrane lipid asymmetry can induce ordered domain formation [43]. Vice versa, the presence of asymmetry can be expected to suppress phase separation. It was also shown that in asymmetric bilayers one liquid-disordered leaflet can strongly influence the phase state towards reaching phase symmetry [44]. As a result our observations are consisted with reported phenomena.

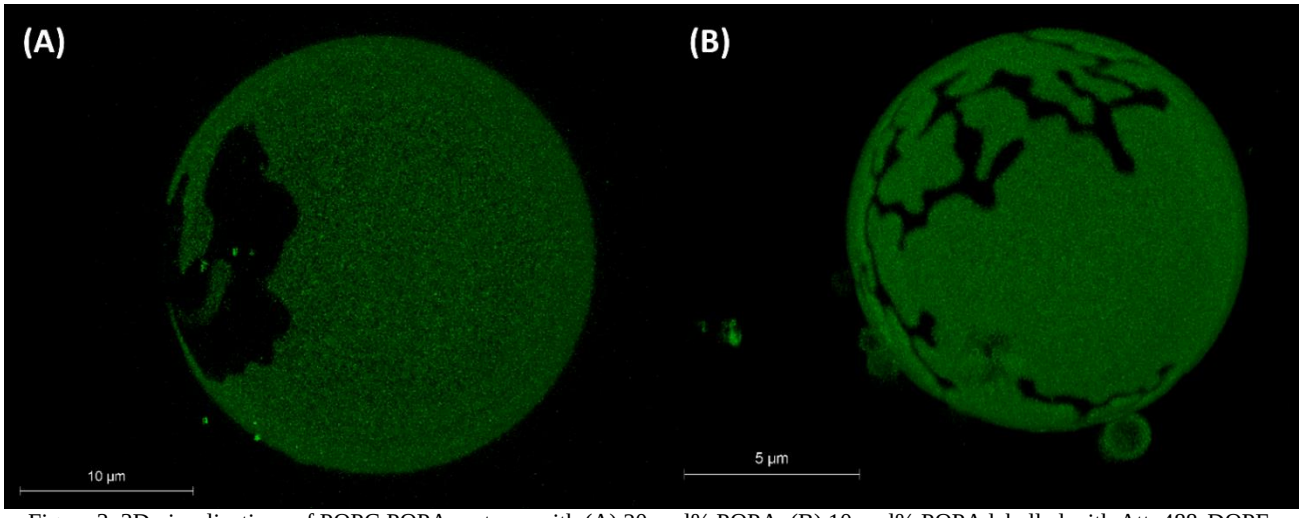


Figure 3. 3D visualizations of POPC:POPA systems with (A) 20 mol% POPA, (B) 10 mol% POPA labelled with Atto488-DOPE.

Moreover, similar phenomenon happened when symmetric systems treated with αSyn-mEGFP were visualized. For the symmetric membranes with low fraction of POPA (POPC:POPA 95:5), punctate signal of the protein on the membrane was observed; see Supporting Figure S3. However, for higher POPA fractions (POPC:POPA 90:10 and POPC:POPA 80:20) the protein coverage on the vesicles was homogeneous; see Supporting Figure S3. This observation could imply that at 5% of POPA in the leaflet (corresponding to a total of 2.5% POPA in the membrane), the bilayer asymmetry induced by protein incorporation was not strong enough to inhibit gel domain formation. At this low fraction of POPA, we also expect that the amount of adsorbed protein is small. For higher concentrations of POPA (and by extend greater protein amount on one-side of the vesicle) domain formation is inhibited. This is similar to observed effects with protein cytochrome C [45], where the phase state of symmetric charged membranes exhibiting coexistence of liquid-ordered and liquid-disordered domains was affected by its adsorption. Here, While those

considerations are interesting on their own, the most important conclusion is that symmetric and asymmetric systems differ substantially in lateral lipid organization.

### 3.3. Mechanical properties determination

Apart from characterizing the presence of asymmetry, composition of leaflets as well as lateral organization of the membrane, using micropipette aspiration of GUVs, we measured the membrane area compressibility moduli of the investigated systems (Figure 3). For POPC symmetric vesicles, the stretching elasticity modulus was found equal to $(\mathbf{255 \pm 31})\ \boldsymbol{mN/m}$ and $(\mathbf{249 \pm 35})\ \boldsymbol{mN/m}$ for electroformed and oil-transferred vesicles, respectively. These results are in agreement with both experimental [33, 46, 47] and theoretical [14, 48] literature reports. For POPC:POPA 80:20 symmetric vesicles, the area compressibility was found to be $(\mathbf{487 \pm 35})\ \boldsymbol{mN/m}$ and $(\mathbf{449 \pm 35})\ \boldsymbol{mN/m}$ for electroformed and oil-transferred vesicles, respectively. These results are also in agreement with theoretical reports [14]. In both cases there are no statistically significant difference between the stretching elasticity of vesicles prepared via electroformation and their oil-transferred counterparts. Similar conclusions for anther mechanical parameter, namely the bending rigidity, were reported recently for these two preparation methods [47]. Furthermore, as electroformed vesicles are in much lower osmolality (150 mOsm) compared to the high osmolality condition (700 mOsm) of the vesicles obtained with the phase-transfer method, this also shows that sugar concentration in this range does not influence the stretching elasticity modulus as assessed with micropipette aspiration. This is in agreement with other literature studies, but for a different mechanical parameter [49]. Interestingly, the values we measure for the area compressibility of the asymmetric system with POPC:POPA leaflet on the outside (referred to as outer-PA) were not significantly different from results for symmetric POPC:POPA membranes. Furthermore, results for asymmetric system with POPC:POPA leaflet on the inside (referred to as inner-PA) were statistically significantly higher than the values obtained both for the symmetric POPC:POPA membrane and for membranes with PA only in the outer leaflet (outer-PA). The area compressibility values for outer-PA and inner-PA vesicles were found to be $(\mathbf{451 \pm 35})\ \boldsymbol{mN/m}$ and $(\mathbf{539 \pm 49})\ \boldsymbol{mN/m}$, respectively. The results are summarized in Figure 3B. Results for individual vesicles as well as example snapshots and tension-area expansion plots are presented in Supporting Information Figures S6-S13.

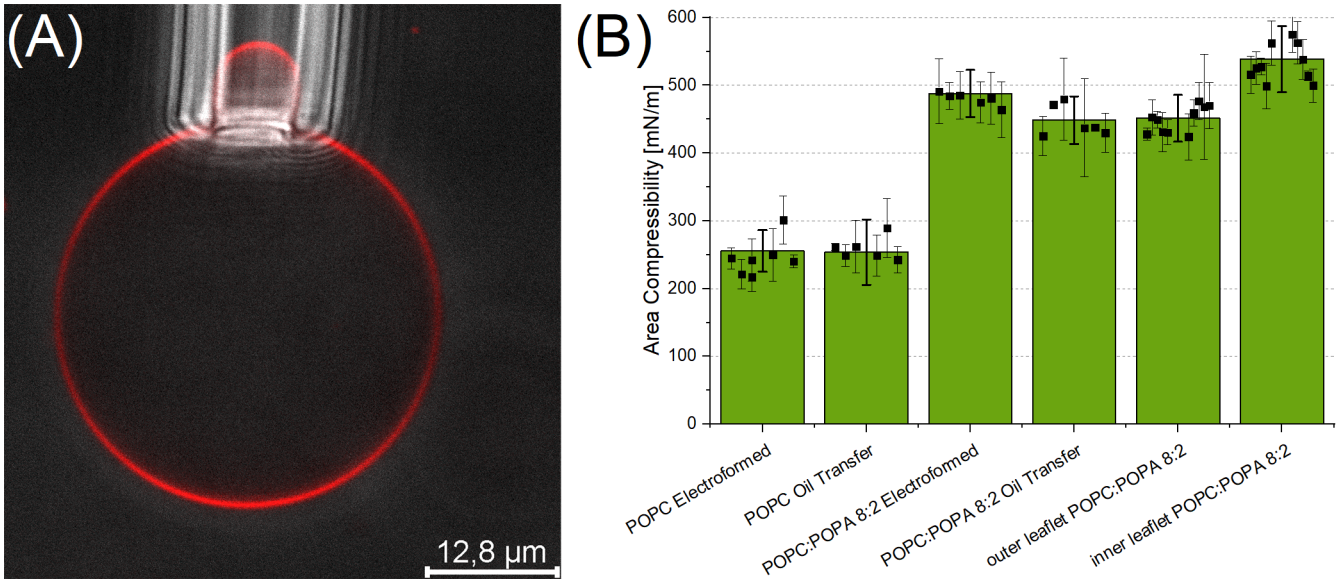


Figure 3. (A) Snapshot of POPC:POPA 80:20 symmetric electroformation system labelled with 0.2 mol% TexasRed during micropipette aspiration experiment. (B) Area compressibility determined for all investigated vesicle systems using micropipette aspiration technique (at least 10 vesicles were measured for symmetric and 15 for asymmetric systems). Several individual measurements for each system are indicated. All measurements were performed in RT (24 °C).

It is not uncommon for asymmetric vesicles to exhibit higher values of the mechanical properties compared to their symmetric counterparts. Such phenomena, namely an increased bending rigidity for the asymmetric membrane containing POPC or DOPC in the opposing leaflets [28, 29] (note that in the explored systems the effect of gravity on the bending rigidity measurements was neglected). Similar effect was also observed for the area compressibility in the case of asymmetric membranes with DMPC or DOPC in the opposing leaflets [30]. However, we are not aware of literature studies showing either data for asymmetric membranes with changed lipids, nor showing difference in the membrane mechanics depending on the positional order of the leaflet composition, namely, whether the inclusion molecule (in our case POPA) is on the outer or on the inner leaflet. Area compressibility of membrane system is defined as a sum of area compressibility of individual leaflets [50], therefore the positional order of the leaflets should not influence the obtained value of area compressibility. This means that both systems – inner-PA and outer-PA – are biophysically different systems. But how exactly? We consider three potential reasons, namely leaflet coupling, compositional differences and differential stress.

A study on much smaller vesicles (100-130 nm) has shown that in the case of other asymmetric POPC:POPE membranes, the localization of POPE in the inner leaflet was energetically preferred and resulted in stronger inter-leaflet coupling [51]. In the reverse situation, when POPE was in the outer leaflet, the coupling was not observed. This coupling had substantial effect on the phase state in each of the leaflets and presence of defects. While the mechanical properties were not discussed in this work, the phase state of the membrane significantly affects the bilayer mechanical properties. One could be tempted to interpret the difference observed here between the stretching elasticity modulus of the inner-PA and outer-PA systems as resulting from similar coupling. However, this work was carried out on large unilamellar vesicles in which the membrane curvature is much higher (~10 $\mu m^{-1}$) compared to that of GUVs (~0.1 $\mu m^{-1}$). Furthermore, POPA and POPE differ in their intrinsic molecular curvatures.

A simpler explanation for the observed results could be a difference between the respective PA concentrations in the inner leaflet of inner-PA vesicles and the outer leaflet of outer-PA GUVs. The higher value of $K_A$ for the inner-PA vesicles would imply higher fraction of PA in their inner leaflet. Indeed, the data for protein intensity as well as zeta potential reflect the outer leaflet composition only and cannot unequivocally confirm the respective fraction of PA in the inner leaflet.

Finally, the difference in membrane elasticity could be related to differential stress, a term introduced with the theoretical model of Hossein and Deserno [52], which describes a state in which differences between the lateral tensions of the two leaflets do not vanish and do not relax over time. In asymmetric bilayers, this differential stress affects the leaflets thermodynamic state and can result in membrane stiffening, i.e. higher bending

rigidity [52]. Here we do not measure the bending rigidity by the stretching elasticity modulus, but as discussed below, these two mechanical parameters are interrelated.

The stretching elasticity modulus $K_A$ is coupled to the membrane bending rigidity κ, and their ratio is quadratically proportional to the membrane thickness (Equation 1) [53-55]:

$$\frac{\kappa}{K_A} = \frac{d^2}{\alpha} \qquad \text{(Eq. 1)}$$

Here, **d** is the hydrophobic thickness of the bilayer and $\boldsymbol{\alpha}$ is the coupling constant. The polymer-brush model predicts α=24 [53], but for completely bound leaflets, it can drop down to α=12 [54] or increase to α=48 for freely sliding monolayers [55]. If we assume a fixed value of the leaflet coupling for the membrane compositions explored here, and have access to values of their thickness, we could make some predictions for the behavior of the membrane bending rigidity. Thus, we employed MD simulations to assess the parameter **d**. A snapshot of the system and density profile are presented in Figure 4A and 4B, respectively. The determined membrane thickness calculated as a distance between the phosphorus atoms in the opposing leaflets $h_{pp}$ for asymmetric system was equal to $(\mathbf{3.92 \pm 0.02})\ \boldsymbol{nm}$ while for symmetric POPC and POPC:POPA 80:20 systems $h_{pp}$ attained the values $(\mathbf{3.78 \pm 0.04})\ \boldsymbol{nm}$ and $(\mathbf{3.92 \pm 0.03})\ \boldsymbol{nm}$, respectively [14]. Remarkably, the membrane thickness was found the same for symmetric POPC:POPA 80:20 and the asymmetric system with only one leaflet containing POPA. The similarity of the hydrophobic thickness of the symmetric and asymmetric POPC:POPA 80:20 membranes and the higher experimentally-determined value of $K_A$ for the latter implies that either the bending rigidity κ increases, or the coupling α decreases. While the increase of bending rigidity for systems exhibiting asymmetry was already reported, this does not explain the difference we observe between inner-PA and outer-PA membranes. Since we don't know whether there is difference in bending in inner-PA and outer-PA systems, this is not sufficient to select the most likely candidate for interpretation of obtained results.

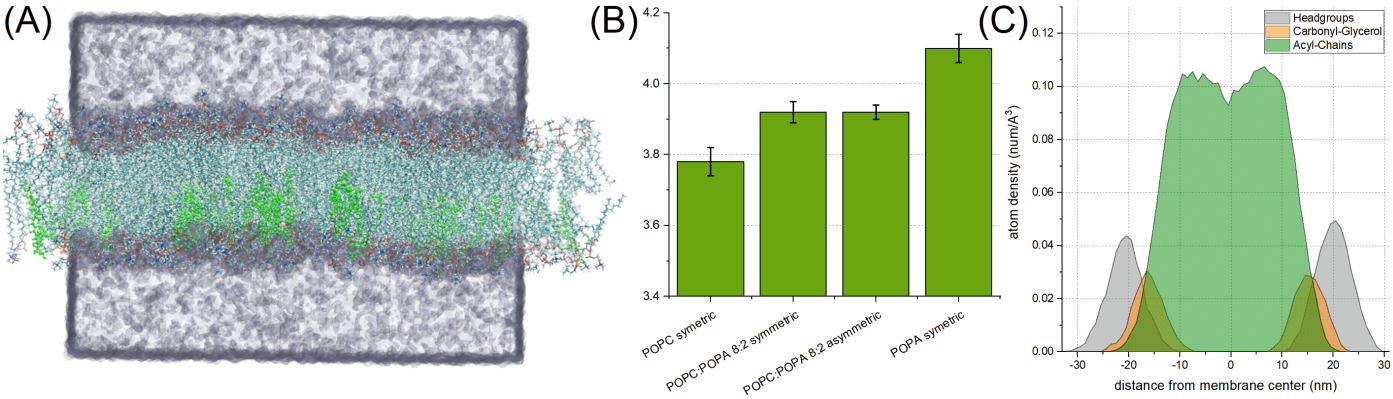


Figure 4. (A) Snapshot of molecular dynamics asymmetric planar membrane system with 20 mol% POPA located only on one of leaflets (the lower one). PA molecules are shown thicker and marked green in the snapshot. (B) Membrane thickness determined for asymmetric system and corresponding symmetric systems from [14]. (C) Density profile of investigated asymmetric system.

## 4. Conclusions

In this work, the effect of leaflet asymmetry in POPA:POPC membranes on their thermodynamic and mechanical properties was investigated. The systems were extensively characterized with fluorescence intensity analysis, binding assay based on the use of the PA-sensor αSyn-mEGFP protein and supported with zeta-potential measurements. We demonstrated that asymmetry was indeed present. The effect of asymmetry on the phase state of the membrane was investigated via confocal microscopy. We provide evidence that gel domains present in the symmetric POPC:POPA systems are suppressed in their asymmetric counterparts. Finally, the mechanical properties of both systems were characterized: the area compressibility was determined using micropipette aspiration technique and the membrane thickness was assessed with molecular dynamics simulations. Asymmetric systems showed higher values of the stretching elasticity and thickness the symmetric POPC:POPA membranes compared to POPC ones. Interestingly, significant difference in the stretching elasticity was observed depending on whether PA was located at the inner or the outer leaflet. We discuss possible interpretations, taking into consideration concepts for potential inter-leaflet coupling, probable difference in the PA fraction in the membrane leaflets as well as stronger differential stress in one of the systems over the other. The experimental data describing this difference is relevant considering the preferential localization of phosphatidic acid to the inner (cytosolic) leaflet of cellular membranes.

## Acknowledgements

This work was possible thanks to the financial support from the National Science Centre (Poland) grant no 2018/30/E/NZ1/00099 (for P.H. and A.C) and Excellence Initiative – Research University (IDUB, Task 12, for D.D.). We also thank Agustin Mangiarotti for helping with setting up micropipette-aspiration setup and Magdalena Zaremba-Czogalla for providing us with pET28 plasmid containing the mEGFP coding sequence.

## References

1. Dimova, R., *Giant Vesicles and Their Use in Assays for Assessing Membrane Phase State, Curvature, Mechanics, and Electrical Properties.* Annu Rev Biophys, 2019. **48**: p. 93-119.
2. Dimova, R. and C. Marques, *The Giant Vesicle Book*. 2019, Boca Raton: Taylor & Francis Group, LLC.
3. Fenz, S.F. and K. Sengupta, *Giant vesicles as cell models.* Integrative Biology, 2012. **4**(9): p. 982-995.
4. Zhu, C., et al., *Giant Unilamellar Vesicle Microarrays for Cell Function Study.* Anal Chem, 2018. **90**(24): p. 14363-14367.
5. Gerstle, Z., R. Desai, and S.L. Veatch, *Giant Plasma Membrane Vesicles: An Experimental Tool for Probing the Effects of Drugs and Other Conditions on Membrane Domain Stability.* Methods Enzymol, 2018. **603**: p. 129-150.
6. Grimmer, M. and K. Bacia, *Giant Endoplasmic Reticulum vesicles (GERVs), a novel model membrane tool.* Sci Rep, 2020. **10**(1): p. 3100.
7. Zhang, W., X. Wang, and X. Han, *Multilayer giant unilamellar vesicles as a model of artificial tissue for drug screen.* Chemical Physics Letters, 2019. **717**: p. 34-37.

8. Kahya, N., *Protein-protein and protein-lipid interactions in domain-assembly: lessons from giant unilamellar vesicles.* Biochim Biophys Acta, 2010. **1798**(7): p. 1392-8.
9. Lorent, J.H., et al., *Plasma membranes are asymmetric in lipid unsaturation, packing and protein shape.* Nat Chem Biol, 2020. **16**(6): p. 644-652.
10. van Meer, G., G.W. Voelker Dr Fau - Feigenson, and G.W. Feigenson, *Membrane lipids: where they are and how they behave.* (1471-0080 (Electronic)).
11. Levental, I. and E. Lyman, *Regulation of membrane protein structure and function by their lipid nano-environment.* Nature Reviews Molecular Cell Biology, 2022.
12. Zegarlinska, J., et al., *Phosphatidic acid - a simple phospholipid with multiple faces.* Acta Biochim Pol, 2018. **65**(2): p. 163-171.
13. Zhukovsky, M.A., et al., *Phosphatidic acid in membrane rearrangements.* FEBS Lett, 2019. **593**(17): p. 2428-2451.
14. Drabik, D. and A. Czogalla, *Simple Does Not Mean Trivial: Behavior of Phosphatidic Acid in Lipid Mono- and Bilayers.* Int J Mol Sci, 2021. **22**(21).
15. Gascard, P., et al., *Asymmetric distribution of phosphoinositides and phosphatidic acid in the human erythrocyte membrane.* Biochim Biophys Acta, 1991. **1069**(1): p. 27-36.
16. Purow, B., *Molecular Pathways: Targeting Diacylglycerol Kinase Alpha in Cancer.* Clin Cancer Res, 2015. **21**(22): p. 5008-12.
17. van Baal, J., et al., *Translocation of diacylglycerol kinase theta from cytosol to plasma membrane in response to activation of G protein-coupled receptors and protein kinase C.* J Biol Chem, 2005. **280**(11): p. 9870-8.
18. Trauble, H. and E. Grell, *Carriers and specificity in membranes. IV. Model vesicles and membranes. The formation of asymmetrical spherical lecithin vesicles.* Neurosci Res Program Bull, 1971. **9**(3): p. 373-80.
19. Szoka, F., Jr. and D. Papahadjopoulos, *Comparative properties and methods of preparation of lipid vesicles (liposomes).* Annu Rev Biophys Bioeng, 1980. **9**: p. 467-508.
20. Peyret, A., H. Zhao, and S. Lecommandoux, *Preparation and Properties of Asymmetric Synthetic Membranes Based on Lipid and Polymer Self-Assembly.* Langmuir, 2018. **34**(11): p. 3376-3385.
21. Huang, Y., S.H. Kim, and L.R. Arriaga, *Emulsion templated vesicles with symmetric or asymmetric membranes.* Adv Colloid Interface Sci, 2017. **247**: p. 413-425.
22. Pautot, S., B.J. Frisken, and D.A. Weitz, *Engineering asymmetric vesicles.* Proc Natl Acad Sci U S A, 2003. **100**(19): p. 10718-21.
23. Noireaux, V. and A. Libchaber, *A vesicle bioreactor as a step toward an artificial cell assembly.* Proc Natl Acad Sci U S A, 2004. **101**(51): p. 17669-74.
24. Enoki, T.A., et al., *Dataset of asymmetric giant unilamellar vesicles prepared via hemifusion: Observation of anti-alignment of domains and modulated phases in asymmetric bilayers.* Data Brief, 2021. **35**: p. 106927.
25. Scott, H.A.-O., et al., *Model Membrane Systems Used to Study Plasma Membrane Lipid Asymmetry.* Symmetry, 2021. **13**(8): p. 1356.
26. Doktorova, M., et al., *Preparation of asymmetric phospholipid vesicles for use as cell membrane models.* Nat Protoc, 2018. **13**(9): p. 2086-2101.
27. Richmond, D.L., et al., *Forming giant vesicles with controlled membrane composition, asymmetry, and contents.* Proc Natl Acad Sci U S A, 2011. **108**(23): p. 9431-6.
28. Karamdad, K., et al., *Studying the effects of asymmetry on the bending rigidity of lipid membranes formed by microfluidics.* Chem Commun (Camb), 2016. **52**(30): p. 5277-80.
29. Elani, Y., et al., *Measurements of the effect of membrane asymmetry on the mechanical properties of lipid bilayers.* Chem Commun (Camb), 2015. **51**(32): p. 6976-9.
30. Lu, L., et al., *Membrane mechanical properties of synthetic asymmetric phospholipid vesicles.* Soft Matter, 2016. **12**(36): p. 7521-7528.
31. Mizuno, S., et al., *Dioleoyl-phosphatidic acid selectively binds to alpha-synuclein and strongly induces its aggregation.* FEBS Lett, 2017. **591**(5): p. 784-791.
32. Yamada, H., et al., *Characterization of alpha-synuclein N-terminal domain as a novel cellular phosphatidic acid sensor.* FEBS J, 2020. **287**(11): p. 2212-2234.
33. Moga, A., et al., *Optimization of the Inverted Emulsion Method for High-Yield Production of Biomimetic Giant Unilamellar Vesicles.* Chembiochem, 2019. **20**(20): p. 2674-2682.
34. van den Ent, F. and J. Lowe, *RF cloning: a restriction-free method for inserting target genes into plasmids.* J Biochem Biophys Methods, 2006. **67**(1): p. 67-74.
35. Steinkuhler, J., et al., *Charged giant unilamellar vesicles prepared by electroformation exhibit nanotubes and transbilayer lipid asymmetry.* Sci Rep, 2018. **8**(1): p. 11838.
36. Carvalho, K., et al., *Giant unilamellar vesicles containing phosphatidylinositol(4,5)bisphosphate: characterization and functionality.* Biophys J, 2008. **95**(9): p. 4348-60.
37. Philips, J.C., et al., *Scalable molecular dynamics with NAMD.* Journal of Computational Chemistry, 2005. **26**(16): p. 1781-1802.
38. Klauda, J.B., et al., *Update of the CHARMM all-atom additive force field for lipids: validation on six lipid types.* J Phys Chem B, 2010. **114**(23): p. 7830-43.
39. Park, S., W. Im, and R.W. Pastor, *Developing initial conditions for simulations of asymmetric membranes: a practical recommendation.* Biophys J, 2021. **120**(22): p. 5041-5059.
40. Giorgino, T., *Computing 1-D atomic densities in macromolecular simulations: The density profile tool for VMD.* Computer Physics Communications, 2014. **185**(1): p. 317-322.
41. Tarun, O.B., M.Y. Eremchev, and S. Roke, *Interaction of Oil and Lipids in Freestanding Lipid Bilayer Membranes Studied with Label-Free High-Throughput Wide-Field Second-Harmonic Microscopy.* Langmuir, 2018. **34**(38): p. 11305-11310.
42. Caffrey, M. and J. Hogan, *LIPIDAT: a database of lipid phase transition temperatures and enthalpy changes. DMPC data subset analysis.* Chem Phys Lipids, 1992. **61**(1): p. 1-109.
43. Kakuda, S., et al., *Loss of plasma membrane lipid asymmetry can induce ordered domain (raft) formation.* J Lipid Res, 2022. **63**(1): p. 100155.
44. Perez, M.A. and P.A. Beales, *Dynamics of asymmetric membranes and interleaflet coupling as intermediates in membrane fusion.* bioRxiv, preprint (2022): p. doi.org/10.1101/2022.07.31.502218
45. Pataraia, S., et al., *Effect of cytochrome c on the phase behavior of charged multicomponent lipid membranes.* Biochim Biophys Acta, 2014. **1838**(8): p. 2036-45.
46. Drabik, D., et al., *Determination of the Mechanical Properties of Model Lipid Bilayers Using Atomic Force Microscopy Indentation.* Langmuir, 2020. **36**(44): p. 13251-13262.
47. Faizi, H.A., et al., *Bending Rigidity, Capacitance, and Shear Viscosity of Giant Vesicle Membranes Prepared by Spontaneous Swelling, Electroformation, Gel-Assisted, and Phase Transfer Methods: A Comparative Study.* Langmuir, 2022. **38**(34): p. 10548–10557.

48. Drabik, D., et al., *Mechanical Properties Determination of DMPC, DPPC, DSPC, and HSPC Solid-Ordered Bilayers.* Langmuir, 2020. **36**(14): p. 3826-3835.
49. Nagle, J.F., M.S. Jablin, and S. Tristram-Nagle, *Sugar does not affect the bending and tilt moduli of simple lipid bilayers.* Chem Phys Lipids, 2016. **196**: p. 76-80.
50. Nagle, J.F., *Area Compressibility Moduli of the Monolayer Leaflets of Asymmetric Bilayers from Simulations.* Biophys J, 2019. **117**(6): p. 1051-1056.
51. Eicher, B., et al., *Intrinsic Curvature-Mediated Transbilayer Coupling in Asymmetric Lipid Vesicles.* Biophys J, 2018. **114**(1): p. 146-157.
52. Hossein, A. and M. Deserno, *Spontaneous Curvature, Differential Stress, and Bending Modulus of Asymmetric Lipid Membranes.* Biophys J, 2020. **118**(3): p. 624-642.
53. Rawicz, W., et al., *Effect of chain length and unsaturation on elasticity of lipid bilayers.* Biophys J, 2000. **79**(1): p. 328-39.
54. Evans, E.A., *Bending resistance and chemically induced moments in membrane bilayers.* Biophys J, 1974. **14**(12): p. 923-31.
55. Goetz, R., G. Gompper, and R. Lipowsky, *Mobility and Elasticity of Self-Assembled Membranes.* Physical Review Letters, 1999. **82**(1): p. 221-224.